

# Modeling Real-Time PCR Kinetics: Richards Reparametrized Equation for Quantitative Estimation of European Hake (*Merluccius merluccius*)

Ana Sánchez,\*<sup>†</sup> José A. Vázquez,<sup>‡</sup> Javier Quinteiro,<sup>§</sup> and Carmen G. Sotelo<sup>†</sup>

<sup>†</sup>Grupo de Bioquímica de Alimentos and <sup>‡</sup>Grupo de Reciclado e Valorización de Residuos (REVAL), Instituto de Investigaciones Mariñas (CSIC), C/Eduardo Cabello 6, 36208 Vigo, Spain

<sup>§</sup>Departamento de Bioquímica e Bioloxía Molecular, Facultade de Bioloxía, Universidade de Santiago de Compostela, Santiago de Compostela 15782, Spain

**S** Supporting Information

**ABSTRACT:** Real-time PCR is the most sensitive method for detection and precise quantification of specific DNA sequences, but it is not usually applied as a quantitative method in seafood. In general, benchmark techniques, mainly cycle threshold (*Ct*), are the routine method for quantitative estimations, but they are not the most precise approaches for a standard assay. In the present work, amplification data from European hake (*Merluccius merluccius*) DNA samples were accurately modeled by three sigmoid reparametrized equations, where the lag phase parameter ( $\lambda_c$ ) from the Richards equation with four parameters was demonstrated to be the perfect substitute for *Ct* for PCR quantification. The concentrations of primers and probes were subsequently optimized by means of that selected kinetic parameter. Finally, the linear correlation among DNA concentration and  $\lambda_c$  was also confirmed.

**KEYWORDS:** real-time PCR, hake, *Merluccius merluccius* identification, DNA quantification, mathematical modeling, Richards equation

## ■ INTRODUCTION

The main applications of real-time PCR were directed toward the field of medicine, in particular to gene expression, cancer diagnosis, autoimmune diseases, or identification and quantification of pathogens.<sup>1–4</sup> Nowadays, this technique is also used in other fields, such as food technology,<sup>5</sup> for which it is an essential tool for the detection and quantification of genetically modified organisms (GMO). Another prominent application of this technique, in the food technology area, is species identification, mainly for food products that do not allow morphological identification of the animal or plant food component.<sup>6–11</sup>

In the case of seafood, species identification has been addressed through several DNA techniques such as restriction fragment length polymorphism (RFLP), single-strand conformation polymorphism (SSCP), or forensically informative nucleotide sequencing (FINS).<sup>12,13</sup> However, these methodologies are less effective in the analysis of products in which several species are present. Therefore, it is necessary to apply other techniques, such as real-time PCR, which can resolve this casuistry in a fast, easy, and cheap way.<sup>14–16</sup> Additionally, labeling rules for mandatory declaration of the amount of certain ingredients in foods (EU directive 2000/13/EG) require tools for their identification and quantification. Reports related to species quantification in foods that do not use real-time PCR are quite scarce and always semiquantitative.<sup>17,18</sup> However, real-time PCR seems to be the most suitable method for quantitative purposes.

Spanish markets have traditionally sold the commercial fish species *Merluccius merluccius* (European hake) mostly as a fresh whole fish, whereas other species belonging to the same family (Merlucciidae) are often marketed as frozen products with

different presentations (such as tails, loins, and fillets). Nowadays, some of these species (South African and silver hake) can also be found fresh in European markets. Because *M. merluccius* is the most appreciated species within the *Merluccius* genus and because its market value is higher than that of the other species, some mislabeling or fraud might occur. Therefore, this is a clear example in which the application of real-time PCR would be required to verify seafood species.

In recent years an increasing number of methods for DNA data modeling and software associated with the evaluation of real-time PCR results have been reported.<sup>19–21</sup> However, the most common method used to analyze the experimental data is based on the threshold cycle method. It uses a fluorescence threshold value (*Ct*) within the exponential phase of the amplification curve as benchmark, wherein all of the samples reached the same fluorescence signal, that is, they have the same amount of amplified product but achieved in different reaction cycles.<sup>22</sup>

The *Ct* method is dependent on the subjectivity to establish randomly the *Ct* value in any point of the exponential phase from the fluorescence cycle curve. This is because the comparison of data from different assays is not feasible. This problem limits, in many cases, the reliability of quantitative PCR causing infra- or overestimation errors in the determination of DNA concentration. Thus, the analysis of data from real-time PCR is far from being standardized among different laboratories, equipments, or technicians.

**Received:** January 11, 2013

**Revised:** March 11, 2013

**Accepted:** March 13, 2013

**Published:** March 13, 2013

Table 1. Equations Used To Model the Real-Time PCR Data Obtained from Hake DNA Analysis<sup>a</sup>

Equation	Conventional form	Parameters	Reparameterised form
Logistic (1)	$F = \frac{F_m}{1 + \exp[\mu(b - C)]}$	$C_{50} = b$ $\lambda_c = C_{50} - \frac{2}{\mu}$	$F = \frac{F_m}{1 + \exp\left[2\left(\frac{C_{50} - C}{C_{50} - \lambda_c}\right)\right]}$
Weibull (2)	$F = F_m \left[1 - \exp\left(-\left(\frac{C}{\alpha}\right)^\beta\right)\right]$	$C_{50} = \alpha \sqrt[\beta]{\ln 2}$ $\lambda_c = \frac{C_{50}}{\sqrt[\beta]{\ln 2}} \left(\gamma^{\lambda/\beta} + \frac{e^{-\gamma} - 1}{\beta \gamma^\gamma e^{-\gamma}}\right)$ con: $\gamma = \frac{\beta - 1}{\beta}$	$F = F_m \left\{1 - \exp\left[-\left(\frac{C \left(\gamma^{\lambda/\beta} + \frac{e^{-\gamma} - 1}{\beta \gamma^\gamma e^{-\gamma}}\right)^\beta}{\lambda_c}\right)\right]\right\}$
Richards (3)	$F = \frac{F_m}{\left\{1 + \exp\left[\mu^* (C^* - C)\right]\right\}^a}$	$C_{50} = C^* - \frac{\ln(2^{1/a} - 1)}{\mu^*}$ $\lambda_c = C^* + \frac{1}{\mu^*} \left[\ln a - \left(\frac{a+1}{a}\right)\right]$	$F = \frac{F_m}{\left\{1 + \exp\left[\left(\frac{\ln a - \left(\frac{a+1}{a}\right)}{\lambda_c - C^*}\right) (C^* - C)\right]\right\}^a}$

<sup>a</sup>Definition of parameters is also summarized:  $F$ , fluorescence;  $F_m$ , maximum fluorescence;  $C$ , amplification cycle number;  $b$ , cycle number to achieve the semimaximum fluorescence;  $\mu$ , specific maximum rate of fluorescence increment;  $C_{50}$ , cycle number to achieve the semimaximum fluorescence;  $\lambda_c$ , lag phase or number of cycles necessary to detect fluorescence in the amplification process;  $\alpha$ , position parameter of Weibull equation;  $\beta$ , form parameter of Weibull equation and related to maximum slope of the fluorescence;  $\mu^*$ , specific apparent maximum rate of fluorescence increment;  $C^*$ , position parameter of Richards equation (with four parameters);  $a$ , form parameter of Richards equation and related to maximum slope of the fluorescence.

An alternative is to adjust the fluorescence data obtained throughout the amplification process (number of cycles) using a suitable mathematical model.<sup>23,24</sup> Nonlinear profiles are easily modeled by sigmoid equations that produce an absolute prediction of PCR kinetics. Different models have been used (Gompertz, logistic, Hill, Chapman, etc.), almost always getting good descriptions of the experimental patterns.<sup>25,26</sup> In this last work, the authors propose a very consistent parameter ( $C_{y0}$ ) to replace the use of  $C_t$ . However, the equation of five parameters defined by Guescini et al.<sup>26</sup> is not reparameterized for  $C_{y0}$  with the subsequent difficulty to calculate the confidence intervals and corresponding comparison between samples by statistical tests. However, mathematical modeling of real-time PCR amplification curves from seafood DNA has never been reported.

The aim of the present work was to compare the capacity and goodness of fit from three sigmoid and reparameterized equations (logistic, Weibull, and Richards) to model the real-time PCR data from hake (*M. merluccius*) samples. A significant parameter,  $\lambda_c$ , from Richards' equation was studied as an alternative to substitute the common and most random  $C_t$  parameter. Finally, the primers and probe concentrations for the MMER\_VIC system<sup>15</sup> were optimized using  $\lambda_c$  values.

## MATERIALS AND METHODS

**DNA Extraction.** DNA was isolated from 0.15–0.2 g of frozen or ethanol-preserved muscle from 10 samples of *M. merluccius* and 5 samples of other Merlucciidae species. Tissue disruption and protein digestion were performed in a thermoshaker at 56 °C with 860  $\mu$ L of lysis buffer (1% SDS, 150 mM NaCl, 2 mM EDTA, 10 mM Tris-HCl, pH 8), 100  $\mu$ L of guanidium thiocyanate (5 M), and 40  $\mu$ L of proteinase K (>20 units/mg). Extra proteinase K (40  $\mu$ L) was added to each sample after 3–4 h and left overnight. After digestion, DNA was isolated by employing the Wizard DNA Clean-Up System kit (Promega) by following the manufacturer's instructions. The eluted DNA was quantified by UV spectrometry at 260 nm and with a Quant-iT PicoGreen dsDNA Assay Kit (Invitrogen) for dsDNA quantification in a VersaFluor Fluorometer (Bio-Rad). DNA concentration was adjusted to 12.5 ng/ $\mu$ L for subsequent RT-PCR reactions.

**Real-Time PCR System and Reaction Conditions.** The evaluated real-time PCR system was a Taqman-MGB species-specific system for *M. merluccius* (MMER\_VIC) designed in a previous work.<sup>15</sup> The sequences of the primers and probe are as follows: MMERCR4F (forward), 5'-CATTYTCYTATATTAACCATTTCAGGCAAT-3'; MMERCR5R (reverse), 5'-TGGGTTGACAGGTTAAATACGAGT-AA-3'; and MMERCR6TP (probe), 5'-AGAACATTAACATAAAAAT-TAAACT-3'. The 5' end of the probe was labeled with the fluorescent reporter dye VIC, and the minor groove binding (MGB) was located at the 3' end.

PCR reactions were performed in a total volume of 20  $\mu$ L in a MicroAmp™ fast optical 96-well reaction plate (Applied Biosystems), covered with MicroAmp™ optical adhesive film (Applied Biosystems). Each reaction contained 25 ng of DNA, 10  $\mu$ L of TaqMan Fast Universal PCR Master Mix UNG Amperase (2 $\times$ ). The final forward and reverse primer concentration was 900 nM, 225 nM being the probe concentration. Reactions were run on an ABI 7500 Fast (Applied Biosystems) with the standard thermal cycling protocol: 95 °C for 10 min followed by 40 cycles of 95 °C for 15 s and 60 °C for 1 min. On the other hand, the optimization experiments of forward and reverse primers were performed at 50, 300, and 900 nM.

**Mathematical Models.** Three sigmoid equations (Table 1) were evaluated to model the profiles of fluorescence versus cycle number of PCR amplification. The selected equations are well-known and applied in a wide range of chemical and biological contexts.<sup>23,24,27–30</sup> The formulation of these equations with parameters of clear geometrical and biological meaning (Figure 1 and Table 1) facilitates the perfect description and classification of the experimental tendencies. In addition, the fittings using reparameterized functions help to calculate easily the confidence intervals of the mentioned coefficients. The algebraic steps required to obtain them are described, for the most complex equation (Richards), in the Supporting Information.

**Numerical and Statistical Methods.** The fitting procedures and parametric estimates from the experimental results were performed by minimizing the sum of quadratic differences between the observed and model-predicted values using the nonlinear least-squares (quasi-Newton) method provided by the Solver macro from the Microsoft Excel spreadsheet. The confidence intervals of the best-fit values for the parametric estimates (Student  $t$  test;  $\alpha = 0.05$ ), consistency of the mathematical models (Fisher's  $F$  test;  $p < 0.05$ ), and covariance and correlation matrices were calculated using the SolverAid macro, which is freely available from Levie's Excelseous Web site: <http://www.bowdoin.edu/~rdelevie/excelseous/>.

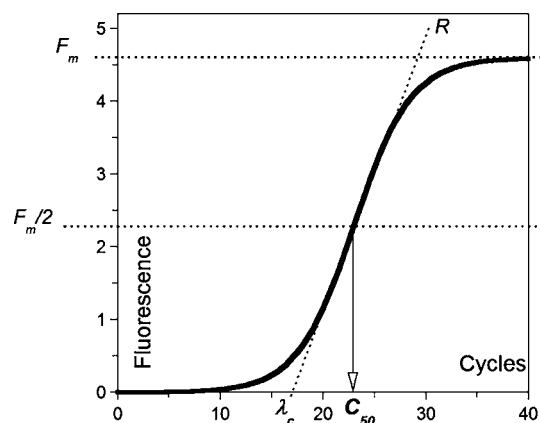


**Figure 1.** Graphical description of the kinetic parameters  $F_m$ ,  $\lambda_c$ , and  $C_{50}$  from a typical sigmoid curve. The line tangent at the inflection point of the sigmoid ( $R$ ) and  $F_m/2$  are also shown.

Subsequently, two criteria based on information theory,<sup>31</sup> the Akaike information criterion (AIC) and the Bayes information criterion (BIC), were used to compare the predictive ability of equations from Table 1 according to the expressions previously described.<sup>32,33</sup>

## RESULTS AND DISCUSSION

**Comparison of Sigmoid Equations To Describe PCR Kinetics.** In Figure 1, the graphical significance of  $F_m$ ,  $\lambda_c$ , and  $C_{50}$  parameters generated by a common sigmoid model are displayed. Two analytical forms (conventional and reparameterised) of the equations tested and the corresponding definitions are summarized in Table 1. The ability of those equations to fit experimental data and describe the profile was evaluated with 10 samples of *M. merluccius*, which are targets of the MMER\_VIC system. Experimental results and fittings to the three models are shown in Figure 2. In all cases, this description was graphically acceptable but a lack of fit was observed at the initial and final phase of amplification curve when eqs 1 and 2 were applied. On the contrary, eq 3 modeled all kinetic phases with perfect agreement between PCR data and theoretical profiles.

Statistical analysis of fittings indicated the validity of the three equations, but revealed that eq 3 generated the best results (Table 2). Using this latter equation, the value of Fisher's  $F$  test was higher than those obtained by eqs 1 and 2. Probability values ( $p$  value) calculated from that test were, in all cases, lower than the significance level established ( $p < 0.001$ ). Furthermore, the goodness of fit defined by the adjusted

**Table 2.** Parametric Estimates and Confidence Intervals ( $\alpha = 0.05$ ) from the Equations Summarized in Table 1 Applied to the Real-Time PCR Data Obtained by the MMER\_VIC System<sup>a</sup>

parameter	eq 1	eq 2	eq 3
$F_m$	<b><math>1.55 \pm 0.06</math></b>	<b><math>1.54 \pm 0.06</math></b>	<b><math>1.67 \pm 0.08</math></b>
$\mu$	$0.28 \pm 0.03$		
$C_{50}$	<b><math>25.48 \pm 0.52</math></b>	<b><math>25.59 \pm 0.52</math></b>	<b><math>25.81 \pm 0.50</math></b>
$\lambda_c$	<b><math>18.44 \pm 0.69</math></b>	<b><math>18.01 \pm 0.70</math></b>	<b><math>17.73 \pm 0.44</math></b>
$\alpha$		$27.60 \pm 0.65$	
$\beta$		$4.84 \pm 0.50$	
$\mu^*$			$0.17 \pm 0.04$
$C^*$			$-10.10$ (NS)
$a$			$303.79$ (NS)
$R^2_{adj}$	0.9925	0.9918	0.9990
$F$ ratio	1602.5	1488.9	4093.9
$p$ value	<0.001	<0.001	<0.001

<sup>a</sup>Statistical values of adjusted coefficient of multiple determination ( $R^2_{adj}$ ),  $F$  ratio, and  $p$  values from Fisher's  $F$  test ( $\alpha = 0.05$ ) are also listed. The most interesting parameters for comparative and descriptive purposes ( $F_m$ ,  $C_{50}$  and  $\lambda_c$ ) are shown in bold. NS, nonsignificant.

coefficient of multiple determination ( $R^2_{adj}$ ) for Richards' function was almost maximal with values of 0.999. The direct comparison between models by means of Akaike and Bayes criteria confirmed the validity of selecting eq 3 as the most appropriate to describe and predict the experimental data (data not shown). In addition, bias and accuracy factors evaluated according to the definitions suggested by Ross<sup>34</sup> were closer to 1 for eq 3, and therefore that equation was more accurate than the others (data not shown).

The estimations of  $\lambda_c$  and  $C_{50}$  parameters were statistically significant (Student  $t$  test;  $\alpha = 0.05$ ), and their values were very similar independent of the model used. The values of  $C_{50}$  were close to 26 cycles, and those of  $\lambda_c$  were about 18 cycles. Nevertheless, the error associated with the confidence intervals was much lower in the estimates produced by eq 3 than those obtained with eqs 1 and 2.

The results of comparison of equations were similar to those reported by Guescini et al.<sup>26</sup> These authors also found that the Richards model was the best candidate to predict the curves generated in mechanisms of real-time PCR (fluorescence vs cycles). However, that equation was formulated with five parameters, whereas eq 3 rejects the intercept coefficient because it is not necessary to model our experimental data set.

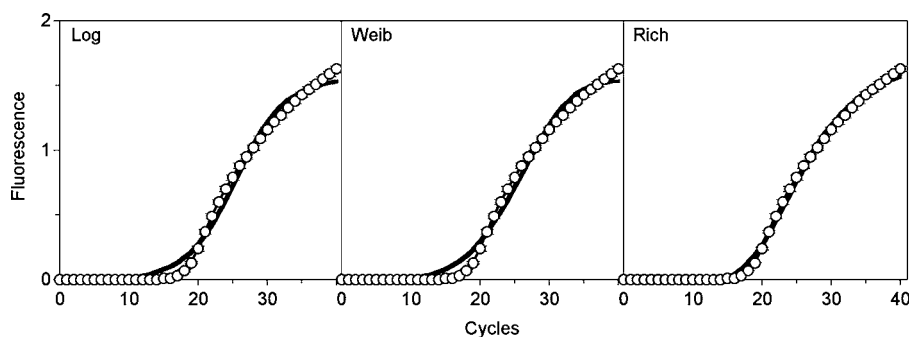


**Figure 2.** Fittings comparisons of sigmoid equations described in Table 1: logistic (Log), Weibull (Weib), and Richards (Rich) using PCR data from *Merluccius merluccius*. In all cases, error bars show the confidence intervals ( $\alpha = 0.05$ ) for  $n = 30$ .

**Table 3. Values of  $C_{50}$  and  $\lambda_c$  Obtained by Fitting to Equation 3 of 10 Samples from *Merluccius merluccius* and 5 Controls without *Merluccius merluccius*<sup>a</sup>**

sample	$C_{50}$	$\lambda_c$	$Ct_{0.055}$	$Ct_{0.1102}$	$R^2_{adj}$	F ratio	p value
MMER1	24.38 ± 0.33	16.70 ± 0.36	17.13	18.15	0.9993	5823.0	<0.001
MMER2	23.07 ± 0.22	17.05 ± 0.28	17.37	18.32	0.9987	7748.7	<0.001
MMER3	23.90 ± 0.21	17.37 ± 0.27	17.65	18.59	0.9988	8158.0	<0.001
MMER4	23.75 ± 0.23	17.00 ± 0.30	17.33	18.26	0.9986	7126.6	<0.001
MMER5	23.39 ± 0.21	16.94 ± 0.25	17.24	18.16	0.9987	7714.5	<0.001
MMER6	23.19 ± 0.21	16.64 ± 0.23	17.00	17.94	0.9987	7682.1	<0.001
MMER7	23.97 ± 0.29	16.83 ± 0.34	17.02	17.98	0.9989	6017.7	<0.001
MMER8	24.82 ± 0.27	17.63 ± 0.30	17.85	18.83	0.9987	7560.8	<0.001
MMER9	23.11 ± 0.20	16.79 ± 0.34	16.99	17.92	0.9988	8383.1	<0.001
MMER10	23.65 ± 0.28	16.42 ± 0.33	16.84	17.81	0.9984	6252.0	<0.001
NO MERR	38.53 ± 0.90	34.10 ± 0.13	34.53	35.57	0.9991	10485.1	<0.001
NO MMER	36.58 ± 0.22	32.17 ± 0.07	32.16	33.12	0.9998	52958.6	<0.001
NO MMER	37.53 ± 0.34	33.18 ± 0.08	33.34	34.31	0.9997	36305.3	<0.001
NO MMER	37.19 ± 0.40	32.91 ± 0.11	33.01	33.97	0.9995	20258.1	<0.001
NO MMER	37.07 ± 0.28	32.52 ± 0.08	32.53	33.52	0.9998	46714.4	<0.001

<sup>a</sup>Confidence intervals were defined for  $\alpha = 0.05$ . Statistical values of adjusted coefficient of multiple determination ( $R^2_{adj}$ ),  $F_{ratio}$ , and  $p$  values from Fisher's  $F$  test ( $\alpha = 0.05$ ) are also summarized as well as the values of  $Ct_{0.055}$  and  $Ct_{0.1102}$  obtained from PCR analysis software.

In addition, the use of nonreparametrized expression makes it difficult to calculate the confidence intervals from kinetic parameters, and therefore the comparison of samples by statistical test of significance was not explored in that work.

**Selection of Best Parameter To Characterize Real-Time PCR Kinetics.** To select between  $\lambda_c$  and  $C_{50}$  as absolute parameter to describe the PCR amplification, an assay using samples of *M. merluccius* (MMER) and other nontarget species (NON MMER), belonging to the family Merlucciidae, was carried out. Parameter estimates and corresponding statistical analysis are shown in Table 3. It is remarkable that no  $R^2_{adj}$  values were inferior to 0.998. MMER samples led to similar estimates of  $\lambda_c$  without significant differences ( $p > 0.05$ ). The average values of  $C_{50}$  and  $\lambda_c$  in MMER\_VIC system ( $23.72 \pm 0.35$  and  $16.94 \pm 0.22$ , respectively) were significantly lower than those observed for nontarget samples ( $p < 0.05$ ) (Table 3). However, although both parameters could be adequately used for describing real-time PCR data, a lower error associated with  $\lambda_c$  has been found, showing that this parameter could be more robust than  $C_{50}$ .

The adequacy of  $\lambda_c$  to substitute for the  $Ct$  value, as the most representative parameter of real-time PCR quantification, was evaluated by comparing two approaches of threshold selection by real-time PCR software (7500 Fast, Applied Biosystems) (Table 3). The  $Ct$  value depends on the threshold level fixed in any point of the exponential phase by the real-time PCR software. Initially, this software establishes the threshold on the basis of the sample that shows the amplification with more delay. Thus, in identification assays with target and nontarget samples, where slight cross-reactions may occur, it is common that the threshold is located in the exponential phase of the amplification curves of the nontarget samples automatically by the software. Therefore, amplification curves of target samples present earlier amplification profiles because the threshold is located prior to its exponential phase. The analysis of real-time PCR data is hence incorrectly performed, and this problem is commonly solved by manual modification of threshold under the arbitrary criterion of the analyst. As can be observed (Table 3),  $Ct$  values calculated with 0.055 and 0.110 thresholds produce differences of 1 unit. Those differences may not be very relevant in studies of species identification, but they

represent a problem in DNA quantification assays because, in this case, small variations in  $Ct$  values generate large differences in DNA concentration (a difference of 1  $Ct$  unit is a 2-fold difference of DNA concentration). Additionally, the confidence intervals of  $Ct$  cannot be defined even when calculated directly from real-time PCR software. This fact generates uncertainty in the definition of the error associated with the  $Ct$  value.

**Optimization of Primers and Probe Concentration (MMER\_VIC system) and Standard Curve Definition Using the Lag Phase Parameter.** The experimental design established to identify the optimal concentrations of forward and reverse primers was performed using different concentrations of primers (50, 300, and 900 nM) and probes (25–225 nM). These optima were selected in the primer concentrations that produced the highest value of maximum fluorescence ( $F_m$ ) and the lowest value of  $\lambda_c$ . The corresponding results are listed in Table 4. The concentrations most suitable for the studied system were 900 and 900 nM.

After the level of primers had been selected, the probe concentration was also optimized with the same criterion. As an example, Figure 3 shows the amplification kinetics with the increase of probe (from 25 to 225 nM). A significant and lineal increase of  $F_m$  was observed with the increase of probe

**Table 4. Values of  $F_m$  and  $\lambda_c$  Obtained by Fitting to Equation 3 from PCR Data Performed for the Primer Concentrations Indicated<sup>a</sup>**

forward (nM)	parameter	reverse (nM)		
		50	300	900
50	$F_m$	0.19 ± 0.00	0.38 ± 0.01	0.46 ± 0.01
	$\lambda_c$	24.39 ± 0.08	24.89 ± 0.11	24.93 ± 0.10
300	$F_m$	0.45 ± 0.01	1.01 ± 0.02	1.14 ± 0.03
	$\lambda_c$	16.73 ± 0.31	17.21 ± 0.25	17.22 ± 0.29
900	$F_m$	0.62 ± 0.02	1.25 ± 0.01	<b>1.53 ± 0.03</b>
	$\lambda_c$	16.01 ± 0.41	17.30 ± 0.15	<b>17.07 ± 0.25</b>

<sup>a</sup>Confidence intervals were defined for  $\alpha = 0.05$ . The most optimal concentrations are given in bold.

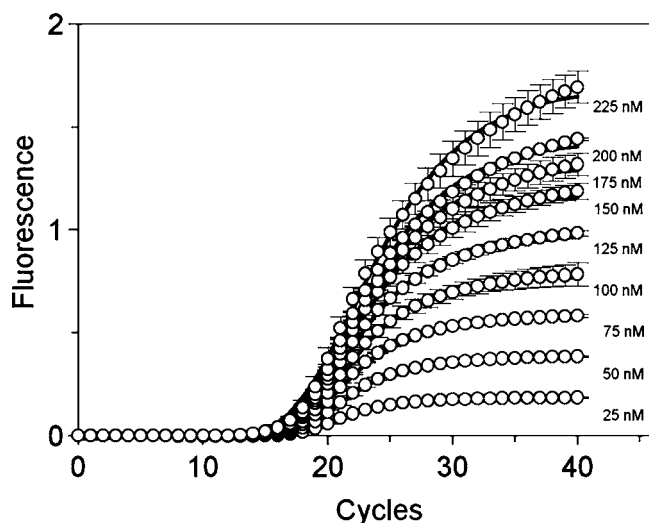


**Figure 3.** Amplification of MMER\_VIC system with several concentrations of probe (25–225 nM) according to the ratios between forward and reverse primers indicated in Table 4. Experimental data were, in all cases, fitted to eq 3. The error bars show the confidence intervals for  $\alpha = 0.05$  and  $n = 3$ .

concentration. These results seem to indicate that an unlimited maximum fluorescence could be achieved with the increase of probe, and therefore its optimum concentration would be larger than the levels studied in the present work. Nevertheless, we have decided to establish, as a compromise option, the optimum concentration of probe as 225 nM to reduce reagent costs.

Finally, amplification curves of MMER\_VIC system were fitted to eq 3 (Figure 4A) with high levels of consistency and great accuracy between experimental and predicted data ( $R^2 > 0.9991$ ). Subsequently, the values of  $\lambda_c$  for each dilution assayed were linearly correlated with the logarithm of the DNA concentration (Figure 4B).

In summary, different sigmoid equations (logistic, Weibull, and Richards with four parameters) consistently fitted the experimental kinetics of real-time PCR using samples of DNA from *M. merluccius*. However, the Richards model was graphical and statistically the best function to describe accurately the amplification data in comparison with the other ones. The formulation of the mentioned equation improved the previously reported one by Guescini et al.<sup>26</sup> due to

reparametrization and construction with only four parameters. The  $\lambda_c$  parameter obtained from the Richards equation was an alternative tool to substitute for the criticized threshold method because it is less sensitive to experimental error, facilitating the calculation of the real confidence intervals of the samples and permitting a more objective comparison between different assays of real-time PCR. The optimization of primer and probe concentrations was thus perfectly performed. Moreover, the relationship among fish DNA concentration and lag phase was accurately defined. Therefore, this method could be used routinely and standardized in the seafood industry and by government institutions to prevent fraud and mislabeling, especially in processed seafood products in which more than one species can be present. This work addressed the specific case of the commercially most appreciated hake species, but it is possible to extrapolate to other commercial fish species.

## ■ ASSOCIATED CONTENT

### 📄 Supporting Information

Algebraic steps required to reparametrize the Richards equation. This material is available free of charge via the Internet at <http://pubs.acs.org>.

## ■ AUTHOR INFORMATION

### ✉ Corresponding Author

\*E-mail: [asanchez@iim.csic.es](mailto:asanchez@iim.csic.es). Phone: +34 986231930. Fax: +34 986292762.

### 📝 Notes

The authors declare no competing financial interest.

## ■ ACKNOWLEDGMENTS

We thank the following companies and research centers that kindly supplied samples: Isla Mar (fishing company), Euro-pacífico (fishing company), Pescanova (fishing company), Natural History Museum and Biodiversity Research Center, University of Kansas (USA), Fisheries and Oceans (Canada), Marine and Coastal Management (South Africa), Northwest Fisheries Science Center (USA), Oviedo University (Spain), Department of Fish Quality, BFEL (Federal Research Center for Nutrition and Food, Germany), and Punto de Inspección Fronteriza (PIF, Spain). We also appreciate the technical assistance received from Isabel Suárez, Helena Pazó, Marta Pérez, and Susana Otero.

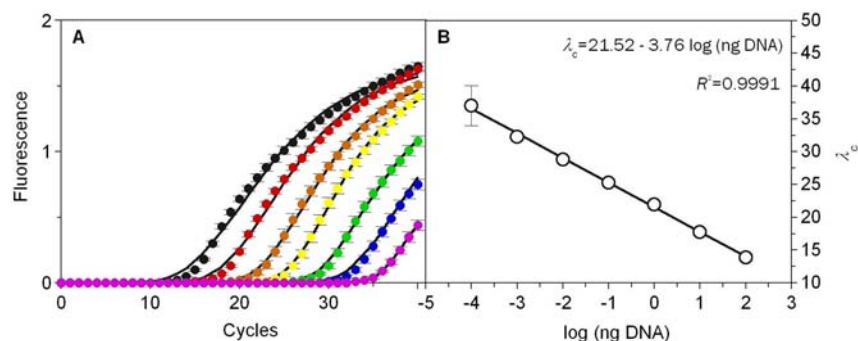


**Figure 4.** (A) Amplifications of MMER\_VIC system for several final concentrations of DNA. Experimental data (points) are fitted to eq 3 (lines). The concentrations of DNA were (in ng) 100 (black), 10 (red), 1 (brown), 0.1 (yellow), 0.01 (green), 0.001 (blue), and 0.0001 (purple). The error bars show the confidence intervals (CI) for  $\alpha = 0.05$  and  $n = 4$ . (B) Linear correlations among  $\lambda_c$  parameter and the logarithm of DNA concentration with the corresponding error bars ( $\alpha = 0.05$ ).

## ■ REFERENCES

- (1) Reischl, U.; Wittwer, C.; Cockerill, F. Rapid cycle real-time PCR methods and applications. *Microbiology and Food Analysis*; Springer: Berlin, Germany, 2001; p 180.
- (2) Wolfgang, D.; Wittwer, C.; Sivasubramanian, N. Rapid cycle real-time PCR methods and applications. *Genetics and Oncology*; Springer: Berlin, Germany, 2002; p 180.
- (3) Deepak, S. A.; Kottapalli, K. R.; Rakwal, R.; Oros, G.; Rangappa, K. S.; Iwahashi, H.; Masuo, Y.; Agrawal, G. K. Real-time PCR: revolutionizing detection and expression analysis of genes. *Curr. Genomics* **2007**, *8*, 234–251.
- (4) Provenzano, M.; Mocellin, S. Complementary techniques: validation of gene expression data by quantitative real time PCR. *Adv. Exp. Med. Biol.* **2007**, *593*, 66–73.
- (5) Levin, R. E. The application of real-time PCR to food and agricultural systems. A review. *Food Biotechnol.* **2004**, *18*, 97–133.
- (6) Brodmann, P. D.; Moor, D. Sensitive and semi-quantitative TaqMan™ real-time polymerase chain reaction systems for the detection of beef (*Bos taurus*) and the detection of the family Mammalia in food and feed. *Meat Sci.* **2003**, *65*, 599–607.
- (7) Hird, H.; Lloyd, J.; Goodier, R.; Brown, J.; Reece, P. Detection of peanut using real-time polymerase chain reaction. *Eur. Food Res. Technol.* **2003**, *217*, 265–268.
- (8) Kesmen, Z.; Gulluce, A.; Sahin, F.; Yetim, H. Identification of meat species by TaqMan-based real-time PCR assay. *Meat Sci.* **2009**, *82*, 444–449.
- (9) Köppel, R.; Dvorak, V.; Zimmerli, F.; Breitenmoser, A.; Eugster, A.; Waiblinger, H. Two tetraplex real-time PCR for the detection and quantification of DNA from eight allergens in food. *Eur. Food Res. Technol.* **2009**, *230*, 367–374.
- (10) Köppel, R.; Ruf, J.; Rentsch, J. Multiplex real-time PCR for the detection and quantification of DNA from beef, pork, horse and sheep. *Eur. Food Res. Technol.* **2011**, *232*, 151–155.
- (11) Mujico, J. R.; Lombardía, M.; Mena, M. C.; Méndez, E.; Albar, J. P. A highly sensitive real-time PCR system for quantification of wheat contamination in gluten-free food for celiac patients. *Food Chem.* **2011**, *128*, 795–801.
- (12) Teletchea, F.; Maudet, C.; Hänni, C. Food and forensic molecular identification: update and challenges. *Trends Biotechnol.* **2005**, *23*, 359–366.
- (13) Lees, M., Ed. *Food Authenticity and Traceability*; Woodhead Publishing: Cambridge, UK, 2003.
- (14) Bertoja, G.; Giaccone, V.; Carraro, L.; Mininni, A. N.; Cardazzo, B. A rapid and high-throughput real-time PCR assay for species identification: application to stockfish sold in Italy. *Eur. Food Res. Technol.* **2009**, *229*, 191–195.
- (15) Sánchez, A.; Quinteiro, J.; Rey-Méndez, M.; Pérez-Martín, R. I.; Sotelo, C. G. Identification of european hake species (*Merluccius merluccius*) using real-time PCR. *J. Agric. Food Chem.* **2009**, *57*, 3397–3403.
- (16) Terio, V.; Di Pinto, P.; Decaro, N.; Parisi, A.; Desario, C.; Martella, V.; Buonavoglia, C.; Tantillo, M. G. Identification of tuna species in commercial cans by minor groove binder probe real-time polymerase chain reaction analysis of mitochondrial DNA sequences. *Mol. Cell. Probes* **2010**, *24*, 352–356.
- (17) Wolf, C.; Lüthy, J. Quantitative competitive (QC) PCR for quantification of porcine DNA. *Meat Sci.* **2001**, *57*, 161–168.
- (18) Marcelino, F. C.; Guimarães, M. F. M.; De-Barros, E. G. Detection and quantification of roundup ready® soybean residues in sausage samples by conventional and real-time PCR. *Cienc. Tecnol. Aliment.* **2008**, *28* (Suppl.), 38–45.
- (19) Jin, N.; He, K.; Liu, L. qPCR-DAMS: A database tool to analyze, manage, and store both relative and absolute quantitative real-time PCR data. *Physiol. Genomics* **2006**, *25*, 25–527.
- (20) Hellemans, J.; Mortier, G.; De Paepe, A.; Speleman, F.; Vandesompele, J. qBase relative quantification framework and software for management and automated analysis of real-time quantitative PCR data. *Genome Biol.* **2007**, *8* (2), R19.
- (21) Pabinger, S.; Thallinger, G. G.; Snajder, R.; Eichhorn, H.; Rader, R.; Trajanoski, Z. QPCR: application for real-time PCR data management and analysis. *BMC Bioinf.* **2009**, *10*, 268.
- (22) Heid, C. A.; Stevens, J.; Livak, K. J.; Williams, P. M. Real time quantitative PCR. *Genome Res.* **1996**, *6*, 986–994.
- (23) Goll, R.; Olsen, T.; Cui, G.; Florholmen, J. Evaluation of absolute quantitation by nonlinear regression in probe-based real-time PCR. *BMC Bioinf.* **2006**, *7*, 107.
- (24) Swillers, S.; Dessars, B.; El Housni, H. Revisiting the sigmoidal curve fitting applied to quantitative real-time PCR data. *Anal. Biochem.* **2008**, *373*, 370–376.
- (25) Rutledge, R. G. Sigmoidal curve-fitting redefines quantitative real-time PCR with the prospective of developing automated high-throughput applications. *Nucleic Acids Res.* **2004**, *32*, e178.
- (26) Guescini, M.; Sisti, D.; Rocchi, M. B.; Stocchi, L.; Stocchi, V. A new real-time PCR method to overcome significant quantitative inaccuracy due to slight amplification inhibition. *BMC Bioinf.* **2008**, *9*, 326.
- (27) Pfaffl, M. W. A new mathematical model for relative quantification in real time RT-PCR. *Nucleic Acids Res.* **2001**, *29*, e45.
- (28) Rutledge, R. G.; Stewart, D. A kinetic-based sigmoidal model for the polymerase chain reaction and its application to high-capacity absolute quantitative real-time PCR. *BMC Biotechnol.* **2008**, *8*, 47.
- (29) Vázquez, J. A.; Murado, M. A. Unstructured mathematical model for biomass, lactic acid and bacteriocin production by lactic acid bacteria in batch fermentation. *J. Chem. Technol. Biotechnol.* **2008**, *83*, 91–96.
- (30) Murado, M. A.; Vázquez, J. A.; Rial, D.; Beiras, R. Dose-response modeling with two agents: application to the bioassay of oil and shoreline cleaning agents. *J. Hazard. Mater.* **2011**, *185*, 807–817.
- (31) Shannon, C. E. A mathematical theory of communication. *Bell Syst. Tech. J.* **1948**, *27*, 623–656.
- (32) Shi, P.; Tsai, C. Regression model selection: a residual likelihood approach. *J. R. Stat. Soc. B* **2002**, *2*, 237–252.
- (33) Vázquez, J. A.; Lorenzo, J. M.; Fuciños, P.; Franco, D. Evaluation of non-linear equations to model different animal growths with mono and bisigmoid profiles. *J. Theor. Biol.* **2012**, *314*, 95–105.
- (34) Ross, T. Indices for performance evaluation of predictive models in food microbiology. *J. Appl. Bacteriol.* **1996**, *81*, S01–S08.
- (35) Vázquez, J. A.; Murado, M. A. Mathematical tools for objective comparison of microbial cultures Application to evaluation of 15 peptones for lactic acid bacteria productions. *Biochem. Eng. J.* **2008**, *39*, 276–287. (Cited in the Supporting Information.)